J Nanostruct 15(1): 1-14, Winter 2025

RESEARCH PAPER

Design and Preparation of Ag_2Se Nanostructures and Investigation of Their Physical and Chemical Properties

Ahmad Abd Al Hussien [1], Kazem Jamshidi-Ghaleh [1], Kahtan A. Mohammed [2], Farzaneh Bayat [1]*

[1] *Department of Physics, Azarbaijan Shahid Madani University (ASMU), Tabriz, 53751 71379, Iran*

[2] *Faculty of Pharmacy, Jabir Ibn Hayyan Medical University, Najaf, Iraq*

ARTICLE INFO

Article History:
Received 05 September 2024
Accepted 23 December 2024
Published 01 January 2025

Keywords:
Ag_2Se Nanomaterials
Chemical properties
Preparation
XRD

ABSTRACT

The ongoing research involves the synthesis of nanocomposites incorporated into polymer materials and investigating their linear, nonlinear, structural, and form optical properties for applications in the field of nonlinear optics. The addition of nanocomposites to polymer materials can enhance and improve many properties, making them appropriate for a wide range of applications. The utilisation of additive nanocomposite manufacturing is highly advantageous in the domain of nonlinear optics (NLO) and its various applications, primarily due to its significant nonlinear response and extensive spectral transparency. Three nanocomposites, namely Ag_2Se+PVA, Ag_2Se+PMMA, and Ag_2Se+PEO, were synthesised using chemical methods. The characterisation of these compounds was performed using XRD, FESEM, EDX, FTIR, RSS, and PL techniques. The UV-VIS spectra were used to study the linear optical characteristics of all the generated samples at various concentrations by adding different polymers. The findings indicated a positive correlation between increasing concentrations and higher absorbance at the same wavelength. Moreover, the Ag_2Se+PVA compound exhibited greater absorption compared to the two preceding compounds. The fluorescence of all generated samples was quantified, and the findings indicated an inverse relationship between concentration and fluorescence, whereby an increase in concentration led to a decrease in fluorescence. The nonlinear calculations involved utilising the Z-Scan technique in two scenarios: open aperture and closed aperture. This was done to determine the values of the nonlinear refractive index (n2) and the nonlinear absorption coefficient (β). The Ag_2Se+PVA compound exhibited superior nonlinear behaviour compared to the two prior compounds. The tests were conducted using a solid-state pump diode laser with a wavelength of 405 nm and a power output of 2.94 mW.

How to cite this article
Al Hussien A., Jamshidi-Ghaleh K., Mohammed K, Bayat F. Design and Preparation of Ag_2Se Nanocomposites and Investigation of Their Physical and Chemical Properties . J Nanostruct, 2025; 15(1):1-14. DOI: 10.22052/JNS.2025.01.001

INTRODUCTION

Nanomaterials science encompasses the process of creating, combining, and analyzing materials that have at least one dimension within the range of 1 to 100 nanometers. The emergence of this field is a direct consequence of the progress made in nanotechnology, enabling us to influence matter at the nanoscale. Nanomaterials have distinctive physical, chemical, and mechanical characteristics that differ from their larger counterparts, rendering them valuable in various applications. Nanomaterials are well-suited for applications such as catalysts, sensors, and energy storage devices due to their very high surface area-to-volume ratio. Moreover, their distinctive optical and electronic characteristics render them valuable in the fields of electronics, photonics, and biological applications [1]. Nanomaterials encompass a

* *Corresponding Author Email: Ahmedmaster915@gmail.com*

wide range of variants, such as nanoparticles, nanotubes, nanowires, and quantum dots. These materials can be synthesised utilising several techniques such as chemical vapour deposition, sol-gel process, and electrochemical deposition. While nanoparticles hold great potential for various applications, there are also legitimate worries regarding their possible environmental and health consequences [2]. Nanomaterials science encompasses the comprehension of the toxicity and potential hazards linked to nanoscale substances. In general, this field is seeing significant growth and offers numerous intriguing opportunities and challenges. Nanomaterials have a considerable impact on optics because of their distinct optical characteristics, which result from their small dimensions and the way their electrical and plasmonic behaviour is influenced by their structure. These materials have the ability to engage with light in innovative manners, which enables the creation of new optical devices and applications [3]. Nanomaterials have significantly influenced the advancement of plasmonics, a field that focusses on the interaction between light and surface plasmons in metallic nanostructures. Plasmonics has facilitated the creation of novel sensor technologies, imaging methodologies, and optical communication systems. Plasmonic sensors that utilize metallic nanoparticles have the ability to detect minute variations in refractive index or molecular binding occurrences. This makes them valuable for identifying biological molecules and other substances of interest. Nanomaterials have also been utilized in optics for the advancement of metamaterials, which are artificially designed structures capable of manipulating light in ways that are not achievable with natural materials. Metamaterials possess negative refractive indices, enabling the creation of flawless lenses and other devices capable of manipulating light in innovative manners [4]. Nanomaterials are utilized in the advancement of novel optical devices, including nanoscale light-emitting diodes (LEDs), which hold promise for applications in displays and lighting. In addition, they are being utilized for the advancement of novel solar cells that exhibit higher efficiency compared to conventional silicon-based solar cells, owing to their capacity to catch a broader range of the solar spectrum. In general, the distinct optical characteristics of nanomaterials have resulted in numerous significant advancements in the areas of spectra and optics. These advancements have the potential to be used in various fields like as sensing, imaging, communications, and energy [3]. In order to fully utilize the nonlinear material, it is necessary to accurately determine and understand its nonlinearity. Various methods exist for analyzing the nonlinearity of materials [3-7]. The z-scan approach, proposed by S. B. Mansoor et al. in 1989, is an easy and precise method [8,9]. The z-scan technique utilizes the detection of spatial distortion in a solitary beam within the nonlinear medium to quantify the nonlinear refractive index, n2. Furthermore, the determination of the nonlinear absorption coefficient β of the medium can be achieved by measuring the transmission of a single light beam as it traverses the nonlinear media, while varying the intensity of the beam. The technique achieves beam intensity change by moving the nonlinear sample across the focal plane of the laser beam [8,9]. The nonlinear refraction is one of the consequences of the real component of the third-order susceptibility of a material. The phenomena described results in the alteration of the laser beam's focus or defocus, depending on the positive or negative value of the refractive index n2. The presence of this non-linear characteristic can be ascribed to various physical factors, which vary depending on the characteristics of the nonlinear medium [10,11]. The importance of the nonlinear refraction and the underlying mechanisms vary depending on the characteristics of the medium. Furthermore, the nonlinear refraction is greatly influenced by the surrounding environment of the nonlinear medium [12,13]. The impact of this phenomenon has been well investigated for several substances [11-15]. The interactions between the solvent and solute, as well as the overall physical properties of the solvent, have an impact on both the type and the extent of nonlinearity shown by the solute. For instance, the polarity of the solvent, its capacity to donate or receive a hydrogen bond, and its thermal properties might alter The nonlinearity of the solute refers to the deviation from a linear relationship between the concentration of the solute and its corresponding property or behavior [11-15].

MATERIALS AND METHODS

Materials

The PVA polymer (Merck,Germany), (kuraray), the PMMA polymer(United Kingdom), (ICI), the

PEO polymer(Germany), the Se element(INDIA), (Central Drug House), the Ag element(Japan)

Methods

The three nanocomposites were synthesized using the following procedure. Initially, we synthesized the three polymers. The PVA polymer was synthesized by introducing 1g of it into 100 mL of deionized distilled water using a homogenizer. Similarly, a solution was prepared by dissolving 1g of PMMA in 100 mL of acetone, and another solution was prepared by dissolving 1g of PEO in 100 mL of deionized distilled water. Next, we synthesized the Ag_2Se nanocomposite by introducing a quantity of (3.14) g of Na_2SeSO_3 to a concentration of (0.98) g of Se. We placed it on the mixer and allowed it to remain there for around 45 minutes, while maintaining a temperature of 90 C within the convection oven. Subsequently, upon subjecting the product to filtration, the colour of the solution transitioned to a white hue. Subsequently, a solution consisting of (0.08) g of $AgNO_3$ and 5 mL of water was prepared and subjected to homogenization until the solution turned white in colour. For the final stage, 5 mL of the prepared Na_2SeSO_3 solution was added to 5 mL of PVA, PMMA, and PEO. This mixture was then combined with 5 mL of previously prepared AgNo3 and placed in a homogenizing device for 15 minutes. The solution was considered complete when its colour turned black. The light sources employed in this study consist of a continuous wave (CW) laser emitting radiation with a wavelength of 405 nm, as well as Gaussian radiation.

RESULTS AND DISCUSSION

Field emission scanning electron microscopy (FESEM)

Typically, the nature of the polymer influences the shape and size of molecules, as longer polymer chains have the ability to coil more extensively, leading to the formation of smaller molecules. Polymers that exhibit strong intermolecular forces likely to undergo chemical

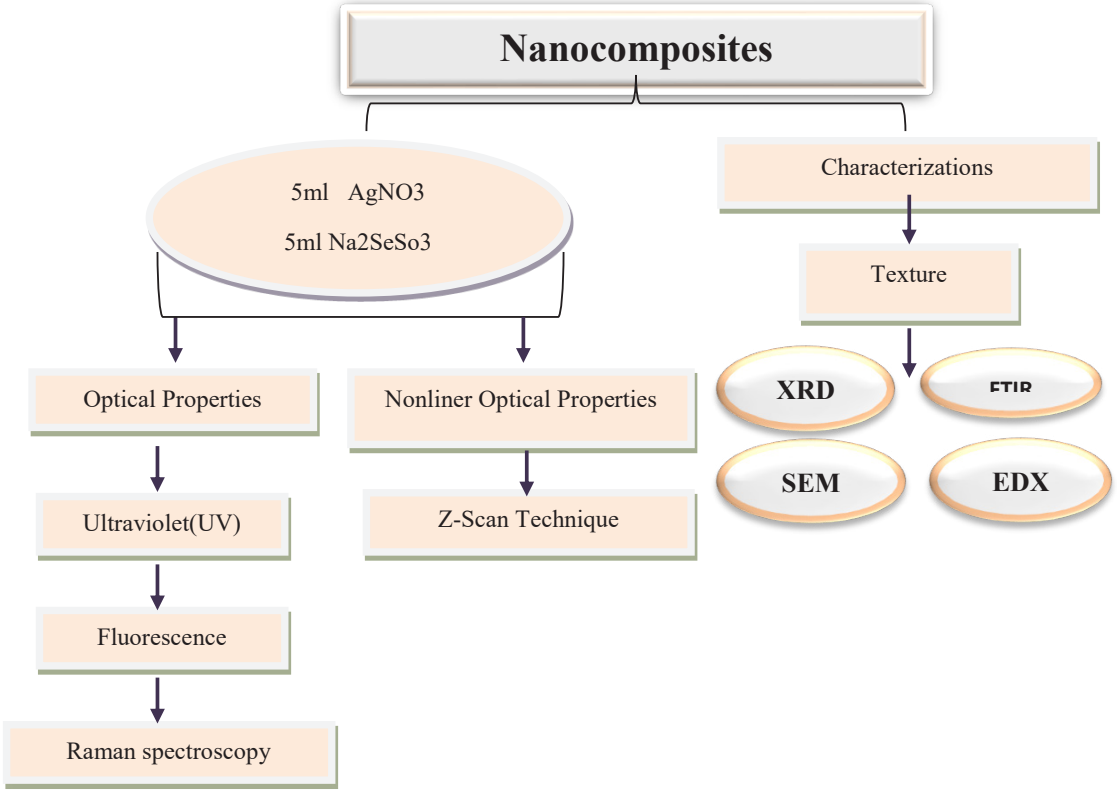

Fig. 1. Shows the experimental procedure as a block diagram of the main steps that are followed in this work.

reactions resulting in the formation of bigger molecules compared to polymers with moderate intermolecular forces. Branched polymers result in molecules with a more non-uniform shape in

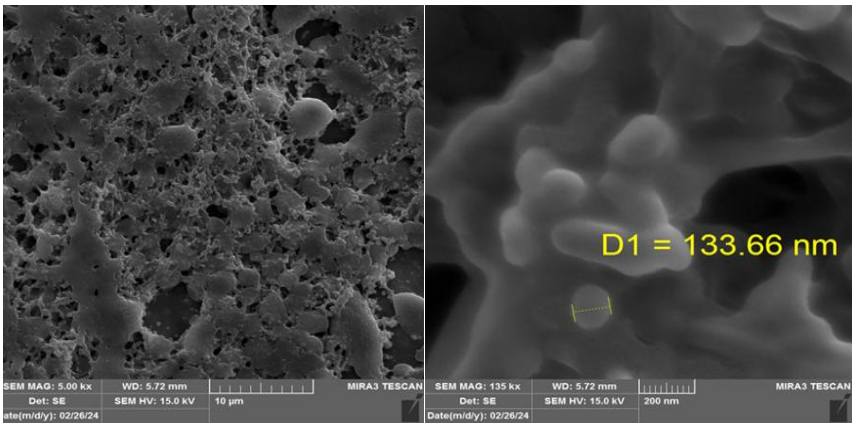

Fig. 2. FESEM image of Ag_2Se+PVA.

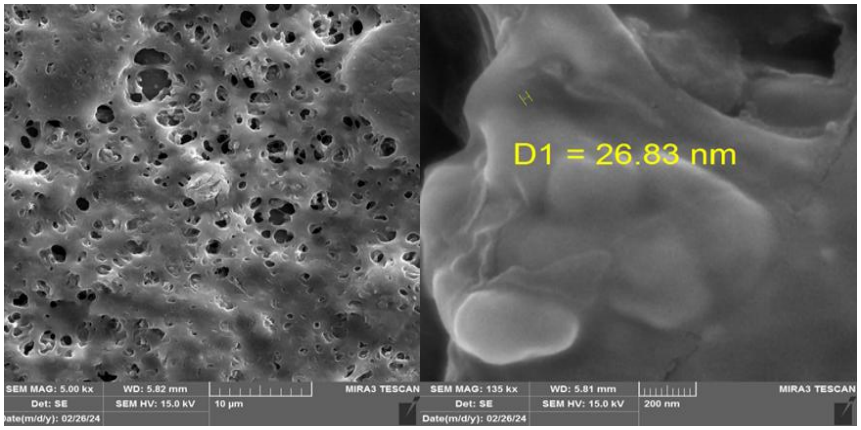

Fig. 3. FESEM image of Ag_2Se+PMMA.

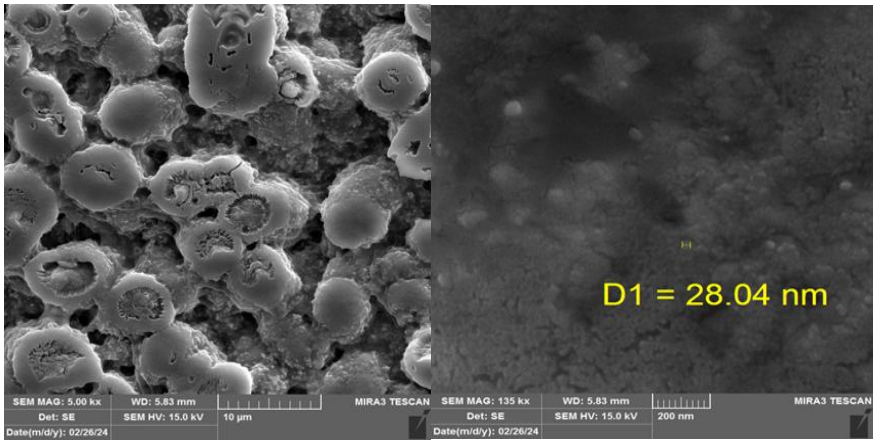

Fig. 4. FESEM image of Ag_2Se+PEO.

comparison to linear polymers. The morphology of Ag_2Se+PVA, Ag_2Se+PMMA, and Ag_2Se+PEO is being studied. The nanocomposites' surface was examined using FESEM. Fig. 2. The surface morphology is characterized by a spherical form and a rough texture. The particles exhibit distinct characteristics, with a wide range of sizes, and an average particle size of approximately 40 nm. Fig. 3 demonstrates that the surface morphology is characterized by a rough and almost spherical shape, as indicated by the uneven and irregular texture of the surfaces. Additionally, the average particle size is approximately 35nm. Fig. 4 depicts a surface that is almost spherical. The roughness of the compound is caused by the interaction between electrons and the uneven surface. The mean particle size is approximately 30 nanometers [12].

EDS Results

To conduct a study on Ag_2Se.An analysis of the materials was conducted to determine their chemical makeup using EDS readings. Figs. 5a and b Display the energy-dispersive X-ray spectroscopy (EDS) spectra of Ag_2Se+PVA and Ag_2Se+PMMA. The EDS signals provide evidence of the existence of selenium, silver, and sodium in the compounds. The substance exhibits three distinct peaks corresponding to the presence of selenium, silver, and sodium. Fig. 5.The provided data displays the energy-dispersive X-ray spectroscopy (EDS) spectra of Ag_2Se+PEO. The EDS patterns validate the existence of selenium and sodium in the compounds. The material exhibits two distinct peaks, one corresponding to selenium and the other to sodium. The three shapes depict a graph that presents the elemental analysis of selenium, silver, and sodium. Table 1 displays the weight composition ratio of Ag_2Se added to PVA, PMMA, and PEO in terms of elemental composition.

Raman Scattering Spectroscopy

The precise frequencies at which the peaks of each band occur were determined using Raman spectroscopy. In order to obtain the most precise Raman spectra, each spectrum was partitioned into three distinct peaks and thereafter examined individually. The low frequency zone is primarily characterized by audio tones, while the medium frequency range involves mixes of audio and optical phonons. Fig. 6 displays the Raman shift of Ag_2Se+PVA nanocomposites.(a) Additionally, there is a concentrated and distinct line spectra at a frequency of 3400 cm^{-1}. The high Raman mode is linked to the vibrations of the C-H and N-H groups. The high vibrational frequencies of these connections are a result of the rapid movement of light atoms with minimal resistance. Fig. 6b The compound Ag_2Se+PMMA exhibits many high-frequency areas consisting of sound phonons with frequencies of 2000, 2400, 2800, 3000, and 3400 cm^{-1}.The intensity of the peaks in the Raman mode varies depending on the vibrations of specific chemical bonds (N-N, C=H2, N=C=O, N=N, C=N, O-H). As the structure of the compound changes, the number and intensity of these peaks increase, indicating a large number of molecular vibrations in the high frequency region. Fig. 6. The compound Ag_2Se+PEO exhibits many high-frequency areas consisting of sound phonons at frequencies of 3100, 3200, 3300, and 3400 cm^{-1}. The intensity of the peaks in the Raman mode varies depending on the vibrations of specific chemical bonds (N=C=O, N=N, C=N, O-H). As the structure of the compound changes, the quantity and intensity of these peaks increase, indicating a significant number of molecular vibrations in the high frequency area [13].

FTIR Spectra results

The FTIR transmission spectrum of Ag_2Se is revealed in Fig. 7a Where the strong bands at 635 cm^{-1} and 1637 cm^{-1} are associated with Vibration and expansion of the benzoinoid and quinoid ring, respectively [14,15].Regions extending over a range of approximately 1500 to 4000 wavenumbers (cm^{-1}).A peak in the range of 2800-3000 cm^{-1} usually indicates the presence of C-H bonds (such as those found in alkanes).

Fig. 7b Regions of high absorption occur at wavelengths:3342.66 cm^{-1}, 1639.54 cm^{-1}, 1369.09 cm^{-1}, 1236.84 cm^{-1}, 1094.68 cm^{-1}, 660.69 cm^{-1}. Absorption occurs because molecules in the sample absorb energy from infrared radiation at these specific wavelengths. This absorbed energy causes the bonds in the molecules to vibrate. The wavenumbers at which absorption occurs depend on the strength and type of the chemical bond, where the peak at 3342.66 cm^{-1} is a broad peak that can be indicative of O-H stretching in alcohols and phenols or N-H stretching in primary amines. The peak at 1639.54 cm^{-1} is a strong peak indicating C=O stretching in different functional groups such as ketones, aldehydes, carboxylic

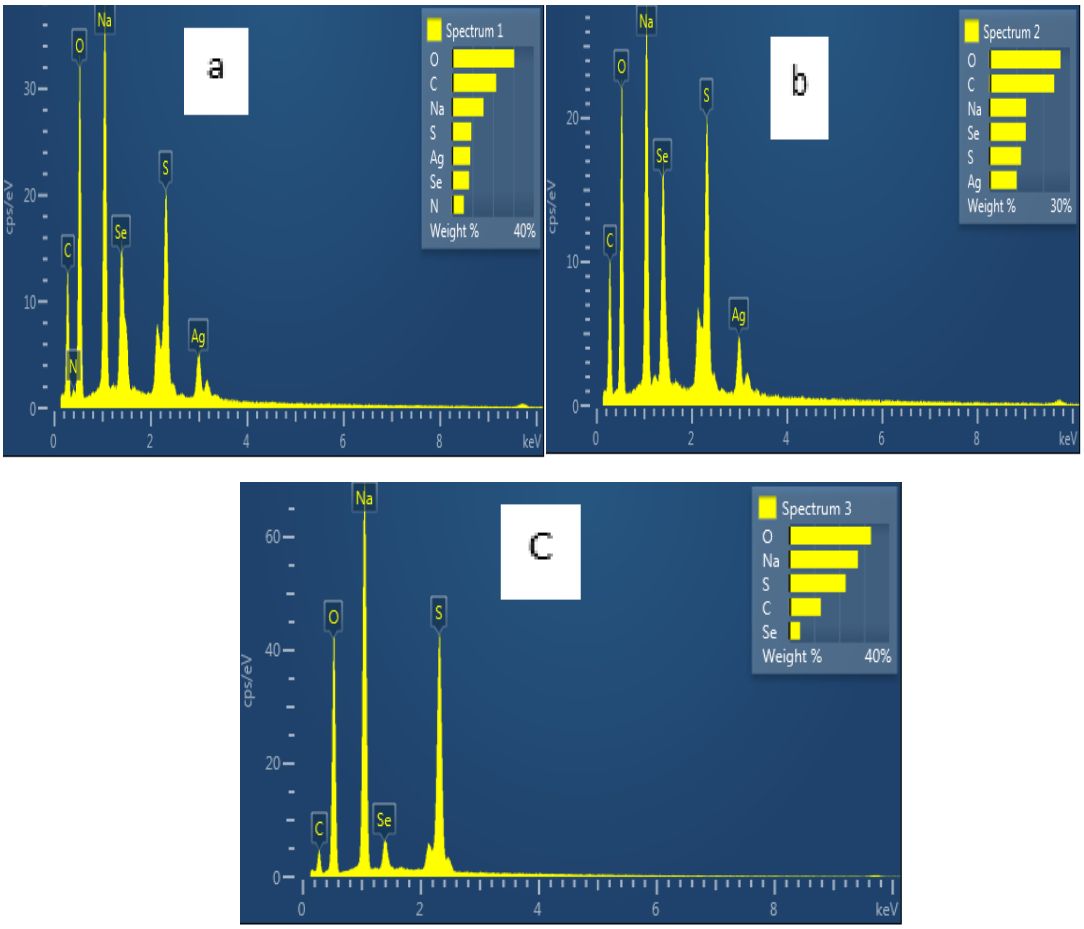

Fig. 5. (a)Typical EDX spectra of Ag_2Se+PVA, (b) Ag_2Se+PMMA, and (c) Ag_2Se+PEO

Table 1. Weight of element composition % of EDS resulting from Ag_2Se added to PVA, PMMA, PEO

Element	Ag_2Se+PVAw%	Ag_2Se+PMMAw%	Ag_2Se+PEO w%
C	21.63	24.16	12.70
N	5.80	-	-
O	30.44	26.52	32.75
Na	15.40	13.68	27.53
S	9.47	11.83	22.61
Se	8.37	13.60	4.41
Ag	8.90	10.20	-

acids, amides and esters. [16,17].

Fig. 7c High absorption occurs at the wavelength 3259.58 cm^{-1}: This can be due to O-H stretching in alcohols, phenols or carboxylic acids .1634.33 cm^{-1}. This is likely due to C=O expansion in ketones or carboxylic acids .1066.39 cm^{-1}: This may be due to the expansion of carbon dioxide in alcohols or ethers .650.57 cm^{-1}: This is a broad peak that can be due to several things, including C-Br stretching in the haloalkanes. When the energy of a light wave matches the vibrational energy of a bond in a molecule, the molecule can absorb light. This causes the bond to vibrate more intensely. Different bonds vibrate at different frequencies. As a result, different molecules absorb light at different wavelengths in the infrared spectrum. [18,19,20].

XRD results

This technique is employed to determine the characteristics of the crystal structure and primary crystalline phases, as well as the orientation of the materials prepared under specific conditions. It is also used to ascertain certain structural parameters, such as crystal size and full width at half maximum (FWHM). From Fig. 8a X-Ray diffraction for Ag_2Se+PVA, the peak intensity at 2θ=29°There is also diffraction at 2θ=33.5°,41°, The material's crystal structure. The presence of different phases in the material (for example, a

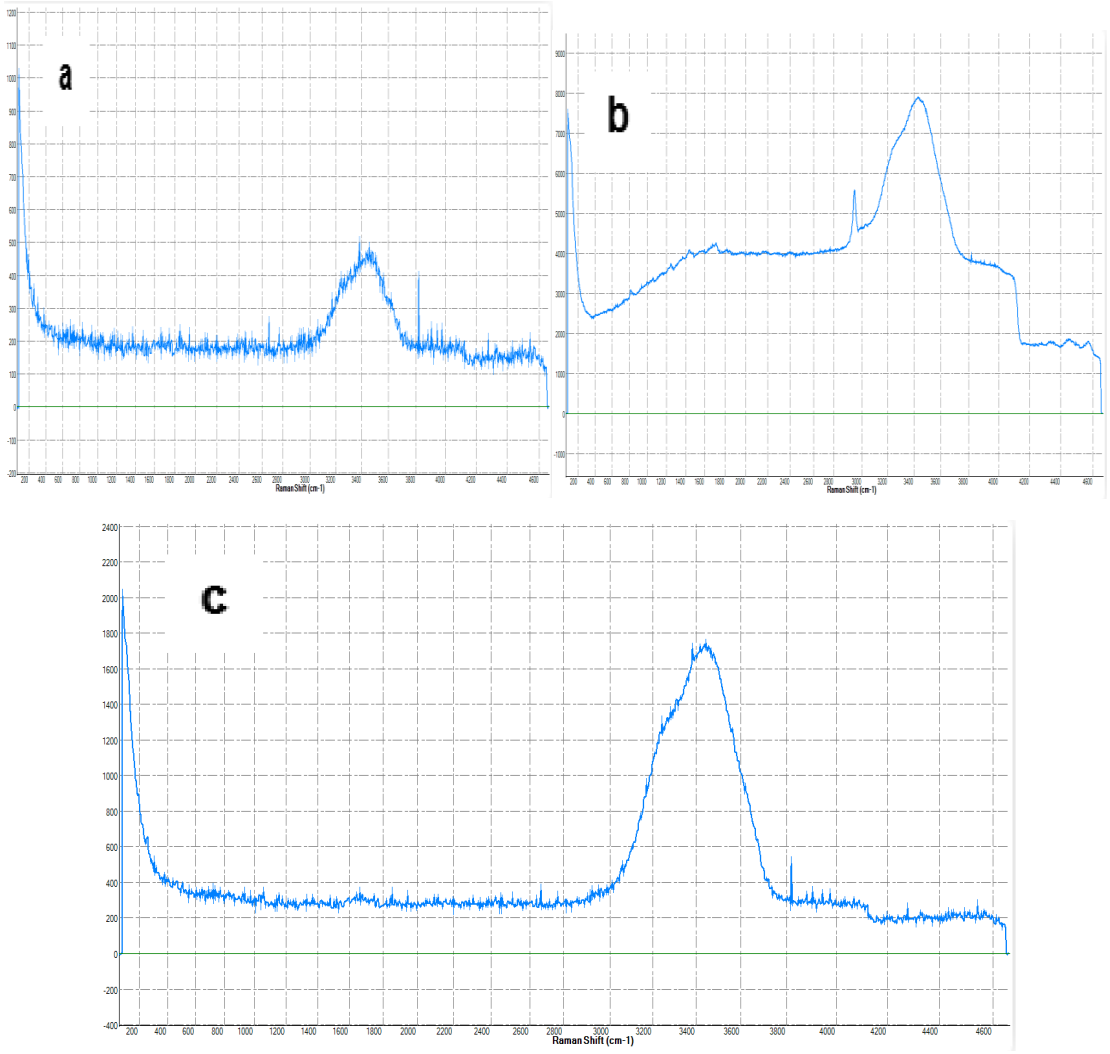

Fig. 6. Raman spectral for (a) Ag_2Se+PVA, (b) Ag_2Se+PMMA, and (c) Ag_2Se+PEO.

mixture of crystalline and amorphous phases) but the most crystalline one is due to the high purity of the material produced. The intensity of the peaks is quite an indicator of the good crystalline nature of the prepared nanoparticles (the size of the individual crystals in a polycrystalline material) and the tension in Article [21]. From Fig. 8b X-Ray diffraction for Ag_2Se+PMMA, Peak intensities at 2θ=28°, intensity of the peaks is quite an indicator of the good crystalline nature of the prepared nanoparticles [22]. Some structural parameters include a crystalline size of about 10 nm and a full width at half maximum (FWHM) of about 0.2°. Narrow peaks indicate that the material is mostly crystalline [23]. From Fig. 8c X-Ray diffraction for Ag_2Se+PEO, the Peak intensity is at 2θ=27.5°, the material present is cubic crystals, and the presence of multiple phases (amorphous and crystalline) can be indicated by broad peaks along with sharp peaks in the XRD, there is a great purity of the produced material, as the intensity of the peak is a complete indicator of the good crystalline nature of the prepared nanoparticles.

Fluorescence Spectra Information

After preparing three compounds and taking the absorption spectra of these compounds when added to different polymers, their emission spectra were recorded using a fluorescence spectrometer. Fig. 9 shows the fluorescence spectra of Ag_2Se added to PVA, PMMA, and PEO polymers. At higher concentrations, the fluorescence intensity reaches a specific value and then decreases with increasing concentration.

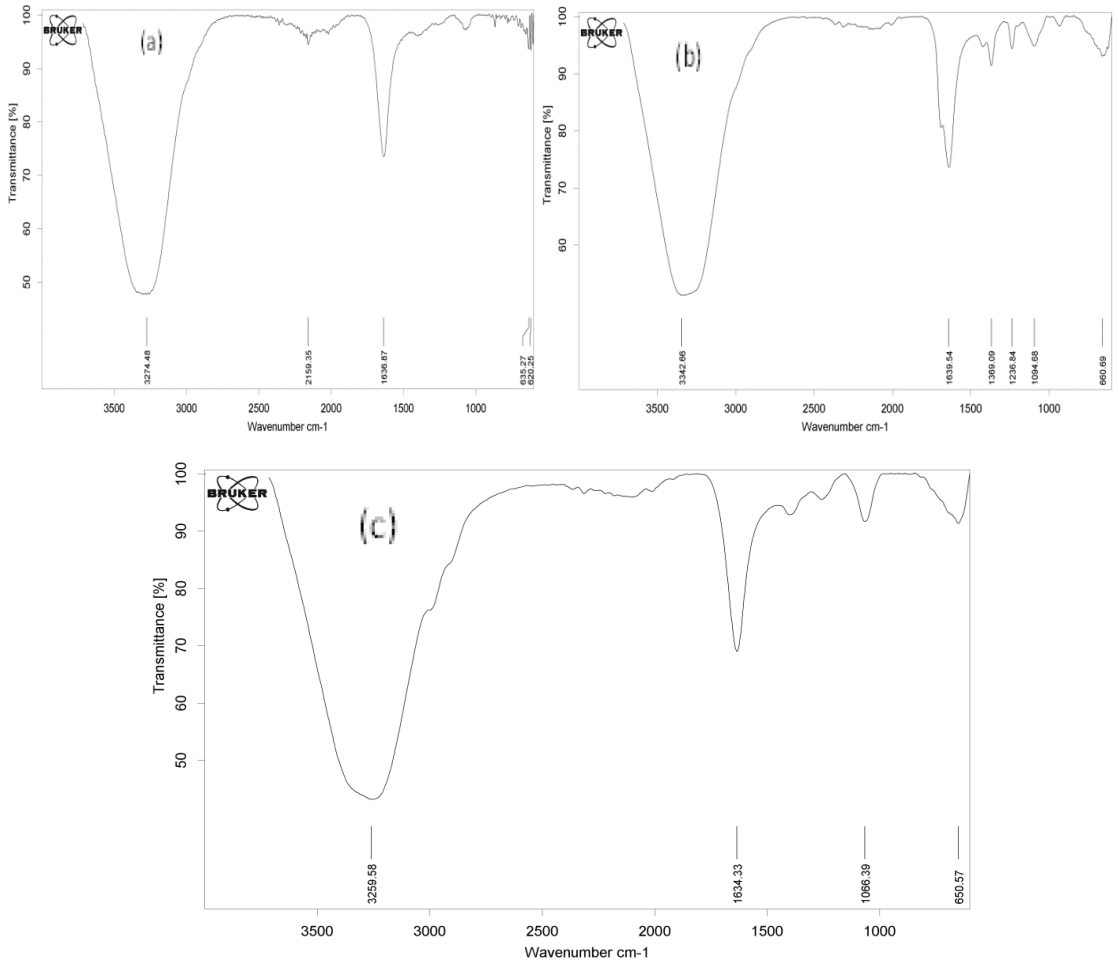

Fig. 7. FTIR spectrum of (a) Ag_2Se+PVA, (b) Ag_2Se+PMMA, and(c) Ag_2Se+ PEO.

This behavior is reported in the literature [24]. Upon adding polymers to silver nitrate, we see a rise in fluorescence intensity, indicating an increase in compound concentration. However, this increase is not sustained. The addition of Ag2Se+PVA results in the production of molecular clumps (aggregations), which subsequently leads to a reduction in the emission spectrum [25]. At low concentrations, the addition of Ag_2Se+PMMA results in strong electronic transitions (S1 to S0), leading to improved fluorescence. This approach is feasible, however, at the maximum concentration, it results in the formation of aggregations among the molecules of the substance. The emission spectrum diminishes due to an escalation in the rate of radioactive decay. From the image, it is evident that as the concentration grows, the peaks of the fluorescence spectra curves shift towards longer wavelengths. Additionally, the width of the fluorescence spectrum increases to a certain extent with increasing concentration, but then starts to decline as the concentration further increases.

Linear Optical Properties

Figs. 10a ,b, c and d) displays the linear absorption spectra of nanocomposite samples. The latest findings indicate that the absorption

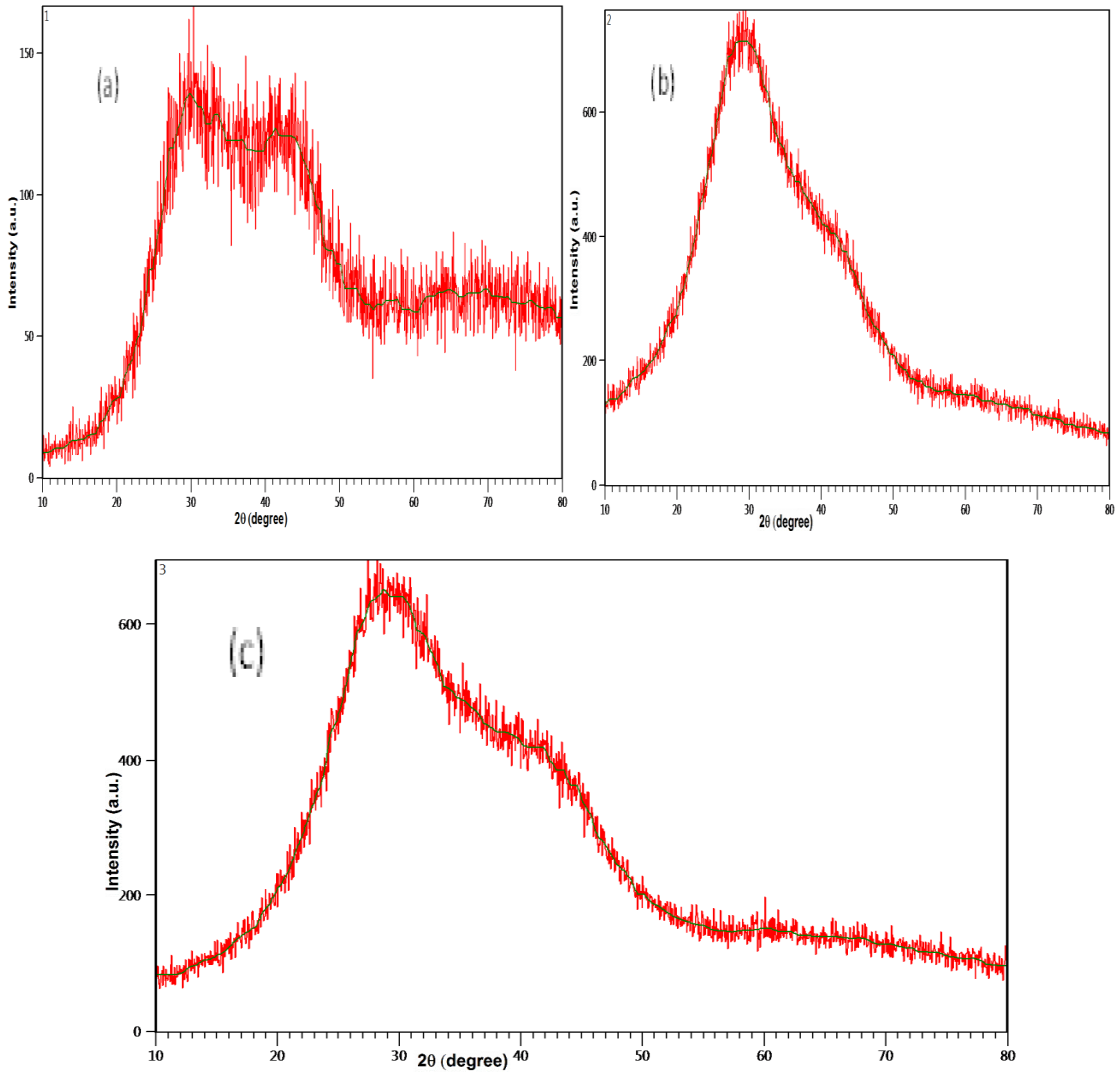

Fig. 8. XRD diffractions pattern for (a) Ag_2Se+PVA, (b) Ag_2Se+PMMA, and(c) Ag_2Se+PEO.

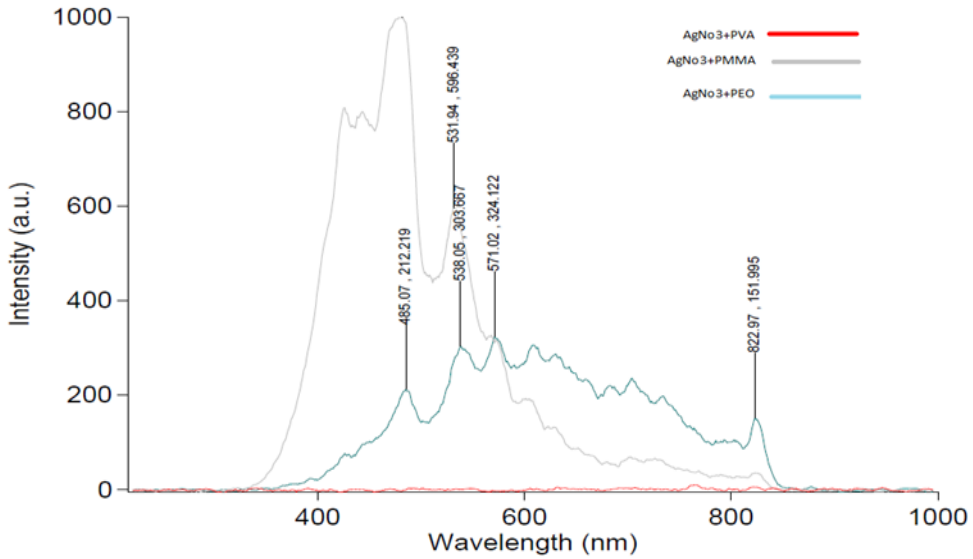

Fig .9. Photoluminescence spectra of Ag_2Se+PVA+PMMA+PEO.

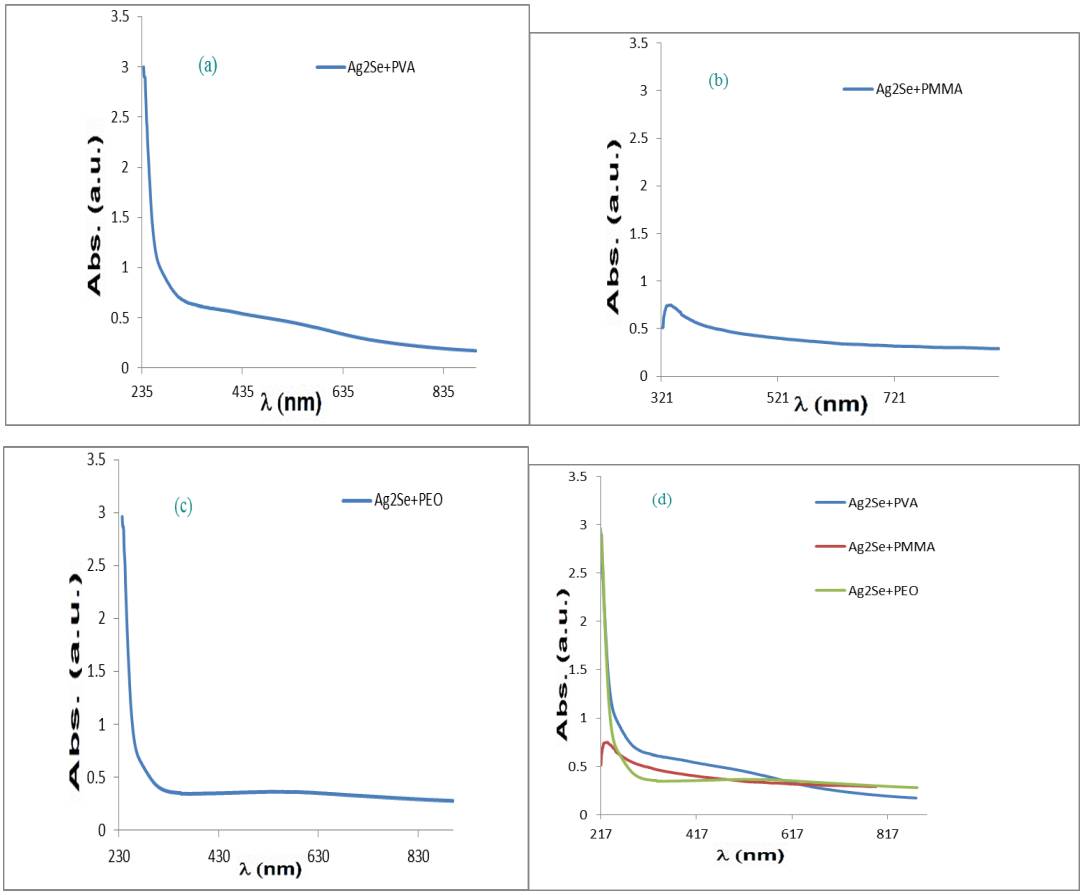

Fig. 10. Absorbance spectra for (a) (Ag_2Se+PVA), (b) (Ag_2Se+PMMA), (c) (Ag_2Se+PEO), and (d) (Ag_2Se+PVA+PMMA+PEO).

peaks exhibited a greater shift towards longer wavelengths when silver selenide (Ag_2Se) was added to PVA compared to when PEO and PMMA were added. The transition is a result of the electronic and vibrational states of the molecules near the interface, causing enhanced absorption of all molecules. The occurrence of nanocomposites in the UV area is considered to be a result of the excitation of high occupied molecular orbital (HOMO) electrons to low occupied molecular orbital (LUMO). The nanocomposite samples exhibit a significant level of absorption in the UV region because the photons possess enough energy to interact with atoms. This interaction causes the electrons to transition from a lower energy level to a higher energy level by absorbing a photon with a certain energy. The primary absorption in absorption spectra signifies the transition between energy bands or excitement. The nanocomposite samples exhibit low absorption values in the visible and near-infrared ranges. This behaviour can be explained by the fact that the energy of the incident photons is insufficient to interact with atoms. As a result, the photons are able to pass through when the wavelength lowers and the energy required for transmission

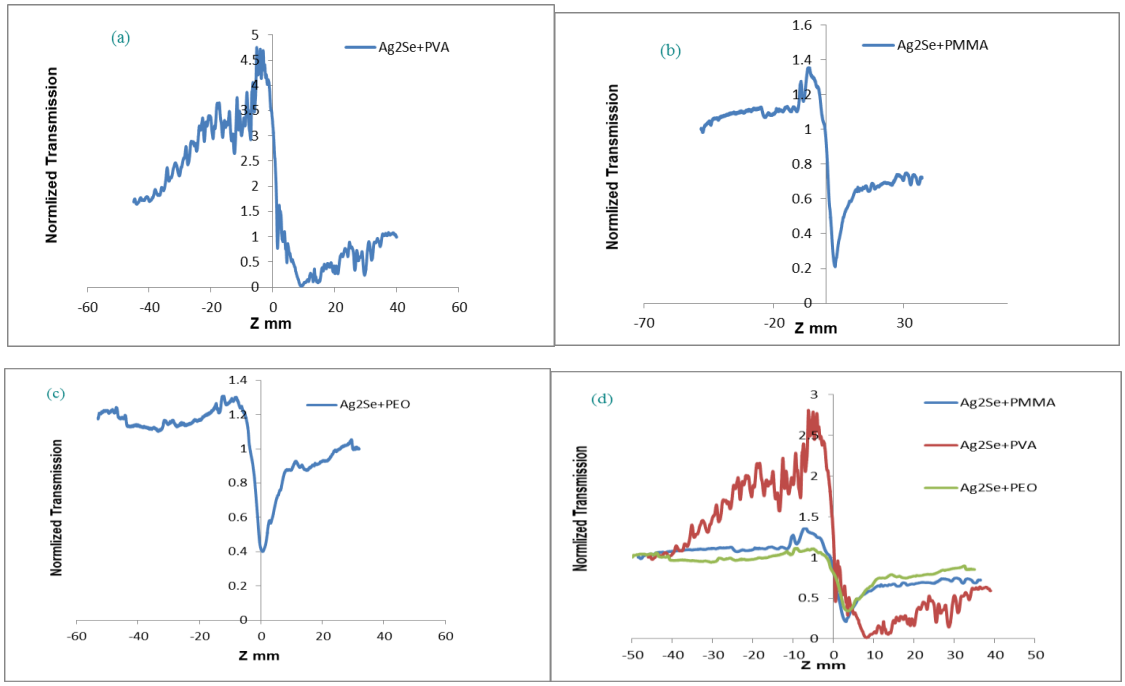

Fig. 11. (a) Z-Scan data for (Ag_2Se+PVA),(b) (Ag_2Se+PMMA),(c) (Ag_2Se+PEO),and(d) (Ag_2Se+PVA+PMMA+PEO).

Table 2. The linear optical parameters at λ=405 nm

Materials	αo (cm^{-1})	Transmittance	Extinction Coefficient	Energy Gap(ev)	Absorption Coefficient
Ag_2Se+PVA	0.967	0.12499	3.83E-06	6.369	2.228
Ag_2Se+PMMA	0.957	30.8906	6.73526E- 07	1.124	0.391
Ag_2Se+PEO	0.170	0.10937	3.90919E-06	6.524	2.273

Table 3. Nonlinear optical parameters

Materials	W.L. (nm)	Power (mW)	I_o (MW/m^2)	α (cm^{-1})	L_{eff} (m)	ΔT	n_2 (m^2/W)	n_o	$R_e\ \chi^{(3)}$ (e.s.u)
Ag_2Se+PVA	405	6.41	43.2348	43.7605	0.000978	1.144371	4.43E-12	1.864076	3.91E-06
Ag_2Se+PMMA	405	3.01	20.3022	39.5989	0.00098	2.8	2.31E-11	1.80098	1.9E-05
Ag_2Se+PEO	405	6.41	43.2348	26.9755	0.00099	0.774876	2.98E-12	1.57833	1.9E-06

reduces [26]. Nanocomposites have superior linear optical characteristics in comparison to non-nanocomposites, which aligns with the findings presented in References [27]. The linear refractive index (NO) and linear absorption coefficient (αo) are two important properties to consider. The absorption coefficients of the first and third silver selenide compounds exceed that of the second compound, as indicated in Table 1.

Non-Linear Optical Properties

The z-scan technique is employed to quantify the nonlinear refractive index and nonlinear absorption coefficient by separately utilising open and closed gaps. Figs. 11a, b, c and d show the normalised permeabilities of Z-Scan measurements for three different combinations: silver selenide added to polyvinyl alcohol (Ag_2Se+PVA), polymethyl methacrylate (Ag_2Se+PMMA), and polyethylene glycol (Ag_2Se+PEO). The nonlinear effect zone spans from -4 mm to 4 mm. The transmittance curve produced from closed-aperture Z-Scan data shows a peak followed by a valley. This suggests that the sign of the nonlinear refractive index is positive (n2 > 0), which leads to the presence of an Autofocusing lens in these samples [28]. When the sample is moved out of focus, the Z-Scan behaviour in the previous figures shows a decrease in the intensity of the transmitted beam, while the transmittance remains rather stable. As the sample moves closer to the beam focus, the intensity of the beam becomes stronger. This causes the sample to undergo self-lensing, which helps align the beam with the aperture in the far field. As a result, the transmittance measured in situ increases. If the beam undergoes any nonlinear phase shift caused by the sample while being moved across the focal zone, the amount of light reaching the detector will change due to self-lensing induced in the material by the powerful laser beam. During sample translation, the detector will measure a signal that exhibits both a peak and a valley. The location of the peak and trough, in relation to the z-axis, is contingent upon the nonlinear phase shift signal. The change in normal permeability from the peak of the curve to the valley (ΔT_(p-v)) The quantity is directly proportional to the magnitude of the nonlinear phase shift that is transmitted on the beam. In addition, when the beam passes via the non-linear media, the ensuing phase shift may occur Can have either a negative or positive value, depending on whether self-focusing or defocusing occurs, In the order mentioned. The magnitude of the phase shift can be determined calculated by measuring the difference in permeability between the highest point and the lowest point. When the beam is concentrated beyond the focal plane, self-defocusing occurs, causing an increase in aberration and broadening of the beam. As a result, the measured transmittance is reduced. When the image is not in focus (Z > 0), the nonlinear refraction is once again minimal, causing the transmittance to be unaffected by Z. The produced materials exhibit two-photon absorption in the open state and self-focusing in the closed state, as seen in previous studies [29,30]. The nonlinear parameters were computed according to the information provided in Tables 2 and 3. The tables demonstrate that the nonlinear parameters for (n2) reduce as concentrations decrease, but the parameter (β) increases with decreasing concentrations. Additionally, the linear parameters (la and αo) decrease as concentrations decrease. This phenomenon occurs as a result of the scarcity of molecules within a certain volume when the concentration is low. The closed-aperture Z-scan method is employed to measure the fluctuating permeability values, which are subsequently utilized to compute the nonlinear phase transformation Δ Φo. The nonlinearity of the Ag_2Se compound is highest when added to the PVA polymer, followed by the PMMA polymer,

and lowest when added to the PEO polymer. This finding is consistent with the reference work [29,30].

CONCLUSION

The Z-Scan approach was used to determine the nonlinear behaviour of all chemicals and successfully prepare nanocomposites. This was done by employing a CW solid-state diode laser pump with a wavelength of 405 nm and a power of 2.94 mW. Ultraviolet and visible spectroscopy was also used and the optical properties were determined. Linearity including transmittance, modulus and refractive index for all samples. Silver selenide nanoparticles were synthesized by chemical method, and silver selenide nanoparticles were examined by Z-Scan, UV, XRD, FESEM, EDX, FTIR, RSS and PL. It was found that it has a linear and non-linear response. From FESEM measurements of nanocomposites, it was found that the average size of nanocomposites ranges between (30-40) nm, so they can be used in the manufacture of highly sensitive nanomaterials as medical thermal sensors. Absorption increases with increasing concentration of the compound, and this agrees well with the Beer-Lambert law, and thus we will obtain good optical properties with increasing concentration of the compound, and this is a suggested behavior for increasing molecules per unit volume. The fluorescence decreases linearly with increasing compound concentration, so these samples can be used in photoelectronic applications. The nonlinear parameters (β) and (n2) have a positive correlation with rising concentrations of compounds. Therefore, compounds at higher concentrations can serve as an efficient laser medium and can be employed for optical limitation purposes. The linear refractive index (no) and linear absorption coefficient (αo) of all samples increase with increasing concentrations. Consequently, these samples can be utilised as resonator cavities in liquid crystal lasers and other optical and photonic devices. The linear optical properties of Ag_2Se+PVA and Ag_2Se+PEO are better than Ag_2Se+PMMA. The Ag_2Se+PVA and Ag_2Se+PMMA nanocomposites give higher nonlinear optical properties than the Ag_2Se+PEO composite.

CONFLICT OF INTEREST

The authors declare that there is no conflict of interests regarding the publication of this manuscript.

REFERENCES

1. Huang T, Hao Z, Gong H, Liu Z, Xiao S, Li S, et al. Third-order nonlinear optical properties of a new copper coordination compound: A promising candidate for all-optical switching. Chem Phys Lett. 2008;451(4-6):213-217.
2. Duerksen KM. Manual of Cutaneous Laser Techniques, 2nd ed. Arch Ophthalmol. 2000;118(11):1595.
3. Maiman TH. Stimulated Optical Radiation in Ruby. Nature. 1960;187(4736):493-494.
4. Hall RN, Fenner GE, Kingsley JD, Soltys TJ, Carlson RO. Coherent Light Emission From GaAs Junctions. Phys Rev Lett. 1962;9(9):366-368.
5. Lamb WE. Theory of an Optical Maser. Phys Rev. 1964;134(6A):A1429-A1450.
6. Ippen EP, Shank CV, Dienes A. Passive mode locking of the cw dye laser. Appl Phys Lett. 1972;21(8):348-350.
7. Shank CV, Ippen EP. Subpicosecond kilowatt pulses from a mode-locked cw dye laser. Appl Phys Lett. 1974;24(8):373-375.
8. Hellwarth RW. Third-order optical susceptibilities of liquids and solids. Progress in Quantum Electronics. 1977;5:1-68.
9. Zel'dovich BY. "Principles of Lasers", by Orazio Svelto, translated from Italian by D. C. Hanna, Plenum Press, New York (1976). Soviet Journal of Quantum Electronics. 1978;8(4):550-551.
10. Laser Physics and Technology. Springer Proceedings in Physics: Springer India; 2015.
11. Symmetries in nonlinear optics. Nonlinear Optics: CRC Press; 2014. p. 115-136.
12. Sampreeth T, Al-Maghrabi MA, Bahuleyan BK, Ramesan MT. Synthesis, characterization, thermal properties, conductivity and sensor application study of polyaniline/cerium-doped titanium dioxide nanocomposites. Journal of Materials Science. 2017;53(1):591-603.
13. O Mousa A, H Nawfal S. Study of Electrical Properties of Photodetector. Journal Electrical Engineering and Science. 2017;3(2):11-18.
14. Lu H-H, Lin C-Y, Hsiao T-C, Ho K-C, Tunney J, Yang D, et al. Nano Fabrication of Conducting Polymers for NO Gas by Dip Pen Nanolithography. 2007 29th Annual International Conference of the IEEE Engineering in Medicine and Biology Society; 2007/08: IEEE; 2007. p. 2253-2256.
15. Peng B, Jungmann G, Jäger C, Haarer D, Schmidt H-W, Thelakkat M. Systematic investigation of the role of compact TiO_2 layer in solid state dye-sensitized TiO2 solar cells. Coord Chem Rev. 2004;248(13-14):1479-1489.
16. Hassan SA, Almaliki MN, Hussein ZA, Albehadili HM, Rabeea Banoon S, Abboodi A, Al-Saady M. Development of nanotechnology by artificial intelligence: a comprehensive review. Journal of Nanostructures. 2023;13(4):915-932.
17. Frayne SH, Barnaby SN, Nakatsuka N, Banerjee IA. Growth and Properties of CdSe Nanoparticles on Ellagic Acid Biotemplates for Photodegradation Applications. Materials Express. 2012;2(4):335-343.
18. Leal-Cruz AL, Vera-Marquina A, Espinoza-Duarte A, Rojas-Hernández AG, García-Juárez A, Aguilar-Martínez JA, et al. Optimization and synthesis approaches of semiconductor nanoparticles of crystalline CdSe using Taguchi method. Journal of Materials Science: Materials in Electronics. 2018;29(18):15801-15807.
19. Thottoli AK, Unni AKA. Effect of trisodium citrate concentration on the particle growth of ZnS nanoparticles.

Journal of Nanostructure in Chemistry. 2013;3(1).
20. Rabeea Banoon S, Mahdi DS, Gasaem NA, Abed Hussein Z, Ghasemian A. The role of nanoparticles in gene therapy: A review. Journal of Nanostructures. 2024;14(1):48-64.
21. Farag AAM, Ashery A, Shenashen MA. Optical absorption and spectrophotometric studies on the optical constants and dielectric of poly (o-toluidine) (POT) films grown by spin coating deposition. Physica B: Condensed Matter. 2012;407(13):2404-2411.
22. Sangamithirai D, Narayanan V, Stephen A. Synthesis and characterization of β-napthalene sulphonic acid doped poly(o-anisidine). AIP Conference Proceedings: AIP Publishing LLC; 2014. p. 1314-1315.
23. Raut BT, Chougule MA, Ghanwat AA, Pawar RC, Lee CS, Patil VB. Polyaniline–CdS nanocomposites: effect of camphor sulfonic acid doping on structural, microstructural, optical and electrical properties. Journal of Materials Science: Materials in Electronics. 2012;23(12):2104-2109.
24. Bykkam S, Kalagadda B, Kalagadda VR, Barray NR, Chidurala SC. A Novel Ultrasonic Assisted Synthesis of Few Layered Graphene/SnO2Nanocomposite and Its Electrochemical Properties. International Journal of Current Research in Science, Engineering and Technology. 2018;1(1):01.
25. Tafulo PAR, Queirós RB, González-Aguilar G. On the "concentration-driven" methylene blue dimerization. Spectrochimica Acta Part A: Molecular and Biomolecular Spectroscopy. 2009;73(2):295-300.
26. Jeyaram S. Nonlinear optical responses in organic dye by Z-scan method. Journal of Optics. 2022;51(3):666-671.
27. Geethu Mani RG, Ahamed MB. Laser performance of rhodamine B and methyl violet B base dye mixture in solid and liquid media. Journal of Nonlinear Optical Physics and Materials. 2014;23(04):1450053.
28. Henari FZ, Patil PS. Nonlinear Optical Properties and Optical Limiting Measurements of {(1Z)-[4-(Dimethylamino)Phenyl] Methylene} 4-Nitrobenzocarboxy Hydrazone Monohydrate under CW Laser Regime. Optics and Photonics Journal. 2014;04(07):182-188.
29. O Mousa A, H Nawfal S. Optical Properties of Porous Silicon Prepared at Different Etching Times. International Journal of Macro and Nano Physics. 2017;2(2):1-5.
30. Atta A, Abdeltwab E, Negm H, Al-Harbi N, Rabia M, Abdelhamied MM. Characterization and linear/non-linear optical properties of polypyrrole/NiO for optoelectronic devices. Inorg Chem Commun. 2023;152:110726.